JACS
JOURNAL OF THE AMERICAN CHEMICAL SOCIETY
Article
pubs.acs.org/JACS

Effect of Acidic Properties of Mesoporous Zeolites Supporting Pt Nanoparticles on Hydrogenative Conversion of Methylcyclopentane

Kyungsu Na,[†,‡] Selim Alayoglu,*[,‡] Rong Ye,[†,‡] and Gabor A. Somorjai*[,†,‡]

[†]Department of Chemistry, University of California, Berkeley, California 94720, United States
[‡]Chemical Sciences Division, Lawrence Berkeley National Laboratory, Berkeley, California 94720, United States

Supporting Information

ABSTRACT: The effect of acidic properties of mesoporous zeolites on the control of product selectivity during the hydrogenative isomerization of methylcyclopentane has been investigated. A series of mesoporous zeolites with controlled acidic properties were prepared by postdealumination process with hydrochloric acid under hydrothermal conditions, and the resultant zeolites used for supporting colloidal Pt nanoparticles (NPs) with a mean size of 2.5 nm (±0.6 nm). As compared to the pure Pt NPs supported on catalytically inert mesoporous silica (MCF-17) as the reference catalyst that can produce isomers most selectively (~80%), the Pt NPs supported on mesoporous zeolites produced C_6-cyclic hydrocarbons (i.e., cyclohexane and benzene) most dominantly. The type and strength of the Brönsted (B) and Lewis (L) acid sites of those zeolites with a controlled Al amount are analyzed by using FT-IR after the adsorption of pyridine and NH_3 temperature-programmed desorption measurements, and they are correlated with the selectivity change between cyclohexane and benzene. From this investigation, we found a linear relationship between the number of Brönsted acid sites and the formation rate for cyclohexane. In addition, we revealed that more Lewis acidic zeolite having relatively smaller B/L ratio is effective for the cyclohexane formation, whereas more Brönsted acidic zeolite having relatively larger B/L ratio is effective for the benzene formation.

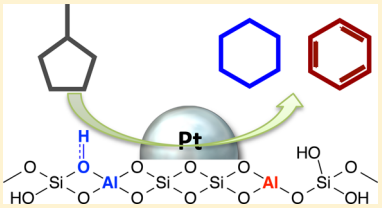

1. INTRODUCTION

Supported metal nanoparticle (NP) catalysts are the typical form of heterogeneous catalysts used ubiquitously in the current chemical industries.[1−5] The surface of a metal NP is the catalytic site on which the reactant can be adsorbed and converted to various product molecules. The molecular interaction to the surface of metal NPs can affect the overall catalytic activity and the product selectivity.[6−9] Size, shape, and composition of metal NPs are also crucial factors for controlling the reaction processes.[6−9] In practical reaction processes, the metal NPs are used as the catalytic sites after supporting on the robust inorganic support materials of porous materials with high surface area and large pore volume.[10−13] Therefore, the structural properties of supporting materials also possess prominent functions that can critically influence the reactions.[14−16]

Among the various porous inorganic materials, zeolites are greatly contributing to the heterogeneous catalytic reactions.[17−19] In current chemical industries, zeolites occupy more than 40% among the whole solid catalysts, which is the largest portion, followed by metal oxides.[17] Zeolites have a charge-localized surface due to the presence of isolated heteroatoms such as Al, Sn, V, and Ti that are covalently surrounded by crystalline microporous silicon oxide framework.[20−22] Zeolites can catalyze many reactions over the charge-localized atomic sites on the zeolite surface that can induce the catalytic reactions through forming an acid−base pair with reactant molecules. Zeolites can usually do the catalysis alone, but they can also make catalytic synergies when metal NPs are supported on them. Such combinations of metal NPs with zeolites make an interface between them, which can sometimes make considerable changes in catalytic activity and product selectivity.[11] Particularly in the viewpoint of product selectivity, achieving 100% product selectivity to a single desired product would become much more feasible through the rational design of catalyst system.[23−25]

In this work, we investigated the effect of acidic properties of zeolite on the control of product selectivity and catalytic activity during model hydrogenative isomerization of methylcyclopentane (MCP). We used mesoporous BEA zeolites having secondary mesopores within nanocrystalline zeolite particles to control the amount and strength of Brönsted and Lewis acid sites for elucidating effects of acidic properties on the selectivity control during the MCP/H_2 reaction under ambient pressure at 150 °C. The acidic properties of mesoporous zeolite were controlled by systematic postdealumination with different concentrations of hydrochloric acid and hydrothermal condition,[26] where 2.5 nm Pt NPs were supported inside mesopore voids with the mean diameter of 15 nm to build catalytic architectures with Pt/zeolite interfaces.

2. EXPERIMENTAL SECTION

Mesoporous BEA zeolite and mesoporous silica MCF-17 were synthesized by following the literature reported elsewhere.[10,27] The

Received: September 8, 2014
Published: November 14, 2014

   dx.doi.org/10.1021/ja509273h | J. Am. Chem. Soc. 2014, 136, 17207−17212

Table 1. Quantification of Acid Sites According to the FT-IR and NH_3 TPD Experiments

					IR			NH_3 TPD			
	BET surface area[a]	pore size[b]	pore volume[c]	Pt[d]	B[e]	L[f]	B/L[g]	L_W[h]	B_W[i]	B_M[j]	B_S[k]
BEA-10	755	20	0.85	0.49	0.98	0.58	1.69	0.568	0.388	0.359	0.247
					(1545)[l]	(1451)[l]		(130)[m]	(196)[m]	(274)[m]	(522)[m]
BEA-4	815	18	0.93	0.51	0.43	0.21	2.05	0.228	0.158	0.145	0.109
					(1548)[l]	(1449)[l]		(123)[m]	(174)[m]	(227)[m]	(550)[m]
BEA-1	770	11	0.86	0.52	0.12	0.04	3.00	0.042	0.038	0.042	0.038
					(1550)[l]	(1448)[l]		(105)[m]	(157)[m]	(187)[m]	(660)[m]
BEA-0.5	865	13	1.23	0.48	0.07	0.01	7.00	0.011	0.024	0.013	0.032
					(1552)[l]	(1447)[l]		(89)[m]	(140)[m]	(198)[m]	(707)[m]

[a]BET surface area calculated by Brunauer–Emmett–Teller method (m^2/g). [b]Average size of mesopore (nm). [c]Total pore volume calculated by BJH method (cm^3/g). [d]Pt loading (wt %) of Pt NPs supported zeolites determined by ICP-AES. [e and f](e) Brönsted and (f) Lewis acid sites (mmol/g). [g]Relative ratio of B/L. [h]Lewis acid sites with weak strength, [i–k]Brönsted acid sites with (i) weak, (j) medium, and (k) strong strength. [l]Center of the IR peak (cm^{-1}). [m]Center of the deconvoluted TPD profile (°C).

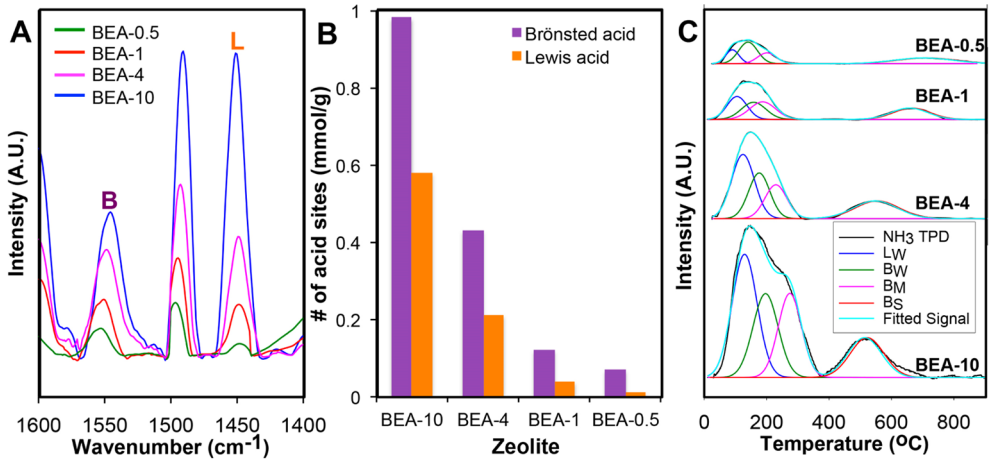

Figure 1. (A) FT-IR spectra after the adsorption of pyridine followed with desorption at 150 °C of BEA-10, 4, 1, and 0.5 (blue, pink, red and green, respectively), where Brönsted (B) and Lewis (L) acid sites are observed at around 1550 and 1450 cm^{-1}, respectively. (B) Quantification of Brönsted and Lewis acid sites of zeolites from FT-IR spectra in (A). (C) NH_3 temperature-programmed desorption (TPD) profiles for BEA-10, 4, 1, and 0.5 (from bottom to top), where each TPD profile was deconvoluted into four distinct peaks of weak Lewis acid sites (L_W, blue) and Brönsted acid sites with weak (B_W, green), medium (B_M, pink) and strong (B_S, red) strengths. The fitted signals from four peaks were also drawn together (cyan).

detailed synthesis procedure was described in the Supporting Information.

For postdealumation of mesoporous BEA zeolite, 0.5 g of H^+-exchanged mesoporous BEA zeolite was diluted in 20 mL of 1–2 M HCl solutions, and heated for 30–90 min under reflux condition. After treatment, the zeolite was collected by filtration, washed with distilled water three times, and dried in an oven at 120 °C. The resultant mesoporous BEA zeolite was denoted as BEA-*x*, where *x* is the content (%) of Al in the zeolite framework.

Poly(vinylpyrrolidone) (PVP)-capped Pt NPs with an average size of 2.5 nm were synthesized by following the literature reported elsewhere (see Supporting Information for details).[16] The PVP-capped Pt NPs were supported on the mesoporous BEA zeolites with controlled Al amount and mesoporous silica MCF-17.

The catalytic materials synthesized in this work were characterized with X-ray diffraction (XRD), transmission electron microscope (TEM), inductively coupled plasma atomic emission spectroscopy (ICP-AES), N_2 physisorption analysis, FT-IR analysis and NH_3 temperature-programmed desorption (TPD). The catalytic testing was performed using lab-build plug-flow reactor connected to a gas chromatograph (GC) equipped with FID detector (see Supporting Information for the details).

3. RESULTS AND DISCUSSION

3.1. Pt Metal NPs Supported Mesoporous BEA Zeolites with Controlled Acidity. Upon postdealumination, Al contents in mesoporous BEA zeolites were systematically controlled. The resultant mesoporous BEA zeolites with controlled amount of Al were further characterized with ICP-AES, XRD, FT-IR, and NH_3 TPD before supporting Pt metal nanoparticles. According to the ICP-AES, the total Al content decreased from 10% to 4%, 1% and 0.5% upon postdealumination. No significant collapse of zeolite framework was observed according to the XRD analysis (see Supporting Information Figure S1A). N_2 adsorption analysis also proved that the series of dealuminated BEA zeolites possessed similar pore properties to the pristine BEA zeolite (see Table 1 for pore analysis data).

The acidic properties of mesoporous BEA zeolites were investigated by FT-IR after the adsorption of pyridine as a probe base molecule and TPD experiments after the adsorption of NH_3 (Figure 1). The IR data shows the stretching bands of pyridine adsorbed on the Brönsted (B) and Lewis (L) acid sites at 1550 and 1450 cm^{-1}, respectively (Figure 1A and Supporting Information Figure S2). The selective quantification of both acid sites was carried out with adsorption coefficients,[28] which

dx.doi.org/10.1021/ja509273h | J. Am. Chem. Soc. 2014, 136, 17207–17212

shows that the number of acid sites decreased proportionally to the total Al contents upon postdealumination (Figure 1B and Table 1). The pristine mesoporous BEA zeolite (BEA-10) showed the largest amount of Brönsted acid sites (0.98 mmol/g) with comparable amount of Lewis acid sites (0.58 mmol/g). The ratio between Brönsted and Lewis acid sites (B/L ratio) is 1.69. The B/L ratio was progressively increased with the decrease of Al contents in the dealuminated BEA zeolites (Table 1). This result indicates that the Lewis acid sites are dealuminated more preferably than the Brönsted acid sites upon hydrochloric acid treatment. As already reported in literatures, the Lewis acid sites are mostly originated from the extraframework Al Species that can be leached out by aqueous acid more easily than Brönsted acid sites surrounded tetrahedrally by −O−Si bonds.[26]

Figure 1C shows NH_3 TPD profiles of mesoporous BEA zeolites, showing the desorption phenomena of NH_3 molecules adsorbed on the acid sites upon increase of temperature. The TPD profiles can be deconvoluted further to four peaks according to the desorption temperature. For example, NH_3 TPD profile of pristine zeolite BEA-10 can be deconvoluted to four peaks at 130, 196, 274, and 522 °C that can be assigned by desorption of pyridine from Lewis acid sites with weak strength (L_W), Brönsted acid sites with weak (B_W), medium (B_M), and strong (B_S) strengths, respectively. Table 1 summarized the quantification results of the series of BEA zeolites from NH_3 TPD profiles in comparison with values calculated by FT-IR. For the analysis of the NH_3-TPD spectra, a protocol was employed in which the calculated B/L ratios form the pyridine-probed FTIR spectra were used as constraints to slave the peak deconvolution (Supporting Information Figure S3).

On the series of BEA zeolite with controlled Al contents, Pt NPs with mean diameter of 2.5 nm were supported. The Pt NPs were synthesized by colloidal synthesis reaction of H_2PtCl_6 precursor salt in ethylene glycol in the presence of PVP as the capping agent (see Supporting Information for details). Prior to catalytic runs, the catalysts were conditioned in 150 Torr O_2 at 250 °C and in 150 Torr H_2 at 150 °C, which were found as the optimum conditions to treat the residual PVP capping and activate Pt NPs.[10] The Pt NPs were supported with good dispersion (Supporting Information Figure S4). In addition, as proved by TEM, the dealuminated mesoporous BEA zeolites have very similar morphology with the pristine mesoporous BEA zeolite (BEA-10) before postdealumination. The crystalline lattice fringes from the microporous zeolite framework were also observed clearly over the zeolite catalysts, which indicated that no significant structural collapse of zeolite framework occurred upon postdealumination with HCl.

3.2. Catalytic Hydrogenative Conversion of Methylcyclopentane. The series of mesoporous BEA zeolites with and without supporting Pt metal NPs was tested for the MCP/H_2 reaction. In Scheme 1, MCP can be converted into various hydrocarbon species via reforming pathways such as dehydrogenation to olefins (1, green), ring-opening isomerization to acyclic isomers (2, pink), ring-enlargement cyclization to cyclohexane (3, blue) or benzene (4, red), and cracking to C_1−C_5 hydrocarbons (5, gray). Figure 2A shows the product selectivity during the MCP/H_2 reaction over the tested catalysts. As shown in Figure 2A, 2.5 nm PVP-capped Pt metal NPs supported on the mesoporous silica (Pt/SiO_2) produced acyclic isomers most dominantly (pink, ~80%) and a lesser amount of olefin products (green, ~20%). Note that the pure mesoporous silica without supporting Pt NPs has no

Scheme 1. Schematic Drawing for the Reaction of Methylcyclopentane Reforming

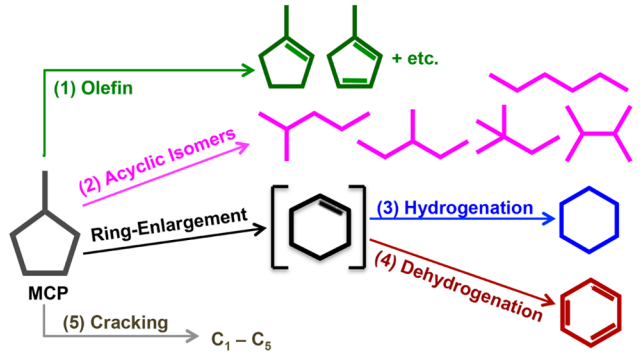

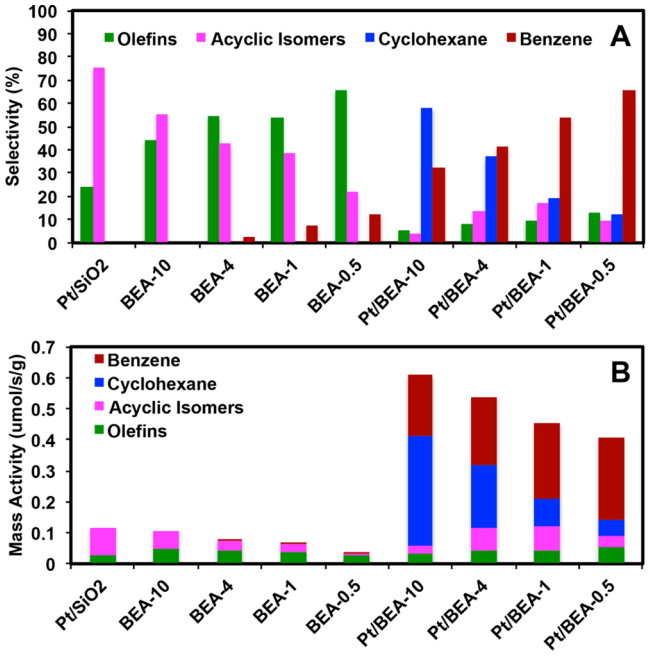

Figure 2. (A) Product selectivity (%) and (B) mass activity data over tested catalysts based on the catalyst weight (μmol/(s/g)).

catalytic activity, and hence Pt/SiO_2 is the catalyst for giving a sole function of Pt NPs for this reaction.

The effect of making catalytic interface between Pt and acid sites on the zeolite surface was investigated after supporting Pt NPs on the series of mesoporous BEA zeolites. In contrast to the Pt/SiO_2, the major products over Pt/zeolites were C_6-cyclic hydrocarbons such as cyclohexane (blue) and benzene (red) that are ring-enlarged products from MCP. It is highly remarkable that such ring-enlarged hydrocarbons were not formed over Pt/SiO_2 at the same reaction condition (150 °C). Benzene can only be produced over Pt/SiO_2 when the reaction temperature approached 250 °C. However, cyclohexane was not obtained over Pt/SiO_2 no matter how the reaction condition was changed. The favorable formation of C_6-cyclic hydrocarbons can be attributed to the synergistic catalytic actions at the interface of Pt and acid sites on the zeolite surface. Interestingly, the relative selectivity ratio between cyclohexane and benzene was progressively changed according to the acidic properties of zeolite supports. Pt/BEA-10 zeolite produced the largest product selectivity to cyclohexane (58%) followed with 32% of benzene. The selectivity to cyclohexane

dx.doi.org/10.1021/ja509273h | J. Am. Chem. Soc. 2014, 136, 17207−17212

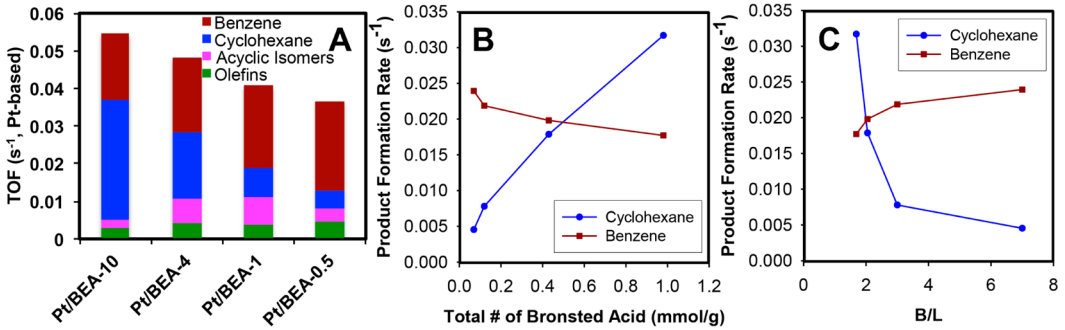

Figure 3. (A) Turnover frequency (TOF, s^{-1}) of Pt NPs supported catalysts. TOFs were calculated based on the number of Pt atoms exposed at the surface of 2.5 nm-Pt NPs, assuming that all the surface Pt sites were reduced at 250 °C under H_2 gas. Each bar is divided into product formation rates for olefins (green), acyclic isomers (pink), cyclization to cyclohexane (blue) and cyclization/dehydrogenation to benzene (red). (B) Correlation of product formation rates (s^{-1}) for cyclohexane (blue) and benzene (red) with the total amount of Brönsted acid sites (mmol/g), and (B) with the relative ratio of Brönsted and Lewis acid sites (B/L).

decreased upon decrease of Al content in the mesoporous BEA zeolite, while the benzene selectivity increased at the expense of cyclohexane decrease. Hence, Pt/BEA-0.5 zeolite produced the largest amount of benzene (65%) with 12% of cyclohexane. This is in similar trend with our previous findings over Pt/MFI catalyst with similar ratios of Al/Si and Pt/Al as the Pt/BEA-0.5 catalyst.[10]

The four pure mesoporous BEA zeolites without supporting Pt NPs were investigated in order to elucidate the sole roles of mesoporous BEA zeolites in the absence of Pt NPs. The results show that these pure zeolites behave like Pt/SiO_2. They could also produce both acyclic isomers (pink) and olefin products (green). The result demonstrated that the role of acidic sites on the zeolite surface is quite similar to the role of Pt NPs, both of which are responsible for dehydrogenation via C−H bond activation and ring-opened isomerization via activations of C−C and C−H bonds. However, the product selectivities toward olefins and acyclic isomers were different depending on the catalyst. BEA-10 zeolite could produce more acyclic isomers, whereas BEA-0.5 zeolite produced more olefins. In addition, small amount of benzene (2.7−12.6%) was also produced over BEA-4, 1, and 0.5 zeolites, where its amount was progressively increased upon the decrease of Al content.

Figure 2B shows the mass activity data for the tested catalysts based on the catalyst weight. The mass activity decreased upon the decrease of Al contents. Pt/BEA-10 showed 0.61 μmol/s/g of total mass activity, which was about six times higher activity than the pure zeolite (i.e., BEA-10). The mass activity decreased to 0.41 μmol/(s/g) for Pt/BEA-0.5, which was also about five times higher activity than pure zeolite (i.e., BEA-0.5). The fact that acyclic isomers and olefin products did not change at any significant rate (see horizontal line in Figure 3A), and the absence of cyclohexane for pure zeolite supports and pure Pt (i.e., SiO_2 is inert) indicates that the reaction could be decomposed into two major pathways: (i) hydrogen extraction and hydrogenative ring-opening over individual Pt and acidic zeolite sites, decoupled from one another; and (ii) hydrogenative ring closure that led to cyclohexene intermediate, not observed in the effluent gas mixture only to be revealed by SFG vibrational spectroscopy,[10] and subsequent hydrogenation/dehydrogenation at the interface of Pt and acidic sites of zeolite.

To elaborate this last conclusion that invokes a multipath chemistry at some dynamic interface, the number densities of acid sites around Pt NPs were calculated for different BEA supports. Monodisperse Pt NPs and uniformly distributed aluminosilicate framework of zeolite could render modeling based on simple geometric variables and physical constraints (i.e., surface area, %Pt loading, NH_3-TPD results) possible (see Supporting Information for details). With this model, the numbers of different acid sites (Lewis and various Brönsted sites) were calculated along the surface plane and in concentric domains away from Pt NP surfaces (Supporting Information Figure S5). It was found that there is, in average, 1 Lewis and 7 Brönsted acid sites within approximately 5 nm of Pt NP surfaces for the BEA-0.5 support (Supporting Information Figure S5A). It should be noted that these numbers are negligibly small as compared to the large number of surface Pt atoms per NP (approximately 250). However, 60 Lewis and 110 Brönsted acid sites were calculated using the same model and identical radial distance for the BEA-10 support (Supporting Information Figure S5D). The implications of this observation are 2-fold. First, the probability that a surface Pt atom would see an acid side of any kind within the bonding vicinity (0−3 Å) is very small in general, and approaches to zero in the case of BEA-0.5. This suggests Pt surface intermediate should spillover to zeolite surface and diffuse several nanometers before encountering, at any significant probability, with any acid site. Second, the changes in overall activity, both mass-based and surface-normalized, are within 30% for the Pt/BEA catalyst for Al concentrations in the 0.5−10% range. This indicates that the ring enlargement chemistry over the zeolites should be the rate-limiting step while the spillover and diffusion processes should be relatively fast. This also implies that the cyclization reaction might still take place on the zeolite support within the bonding proximity of surface Pt atoms.

3.3. Correlation of Acidic Properties with Product Formation Rates. Given the systematic changes in product selectivity between cyclohexane and benzene over the series of Pt/BEA catalysts, one should turn into particular structure−reactivity correlations based on the acidic properties of zeolite supports. To this end, the product formation rates (s^{-1}) were correlated with the number distributions of various acidic sites of different types and strengths; this is illustrated in Figure 3B. It was found that the formation of cyclohexane dramatically increased with increasing the number of Brönsted sites, summed over different strengths, whereas benzene formation showed a slight negative slope. It should be noted that the strengths of various Brönsted sites (weak, medium and strong) were defined in the broadest definition of the term, referring to

dx.doi.org/10.1021/ja509273h | J. Am. Chem. Soc. 2014, 136, 17207−17212

the low, medium and high temperature NH_3 desorption peaks. The relative strengths of various Brönsted sites are, however, different for the Pt/BEA catalysts. In general, strong Brönsted sites increased in strength (i.e., higher desorption temperature of NH_3) in the order BEA-10 < BEA-4 < BEA-1 < BEA-0.5, while weak and medium Brönsted sites decreased in strength in the same order (Figure 1C). Pyridine-probed FT-IR study also indicated an increase in average vibrational frequency of pyridine adsorbed on Brönsted sites from BEA-10 to BEA-0.5 (Figure 1A) and, therefore, corroborated the conclusions drawn from the analysis of NH_3-TPD data. Likewise, the relative strengths of weak Lewis sites increased in the order BEA-0.5 < BEA-1 < BEA-4 < BEA-10, indicated by the NH_3-TPD and pyridine-probed FT-IR results. Therefore, the selectivity switchover from cyclohexane to benzene for the Pt/BEA catalysts (i.e., the ease of hydrogen extraction) could be single-handedly delivered by the presence of strong Brönsted sites, in particular, those that exhibited stronger bonding with the base molecules as in the case of BEA-0.5. In support of this, it should be noted that pure BEA-0.5 led to the formation of benzene in low, yet measurable amounts, while pure BEA-10 did not produce any measurable cyclic isomers.

Alternative to this view, the Lewis acid sites could interact with C═C double bonds, present in either benzene or cyclohexene intermediate, by forming π-complex with aluminum at Lewis acid sites. If correct, this should lead to stronger (weak) Lewis acid sites for the Pt/BEA-0.5 catalyst than the Pt/BEA-10 catalyst. Our findings, however, indicate the opposite trend; the desorption temperature of NH_3 over the Pt/BEA-10 catalyst was higher than that over the Pt/BEA-0.5 catalyst (130 vs 89 °C in Table 1). Furthermore, the number of weak Lewis sites over the Pt/BEA-10 outmatched those over the Pt/BEA-0.5 by 50:1. Nonetheless, it should be noted that we tried and found a correlation between the B/L ratios and formation rate toward benzene; the larger the B/L ratio, the higher the formation rate toward benzene, and vice versa (Figure 3C).

4. CONCLUSION

In conclusion, effect of the acidic properties of mesoporous zeolites supporting Pt NPs has been investigated for the hydrogenative reforming of MCP. The sole Pt NPs and the pure mesoporous zeolites without Pt NPs have similar catalytic functions that can make olefin and acyclic isomer products with different selectivity. However, making catalytic interfaces of Pt NPs with acid sites on the zeolite surface enhanced the activity very significantly and hence lowered the temperature for the formation of C_6-cyclic hydrocarbons by ∼100 °C as compared to the Pt/SiO_2. In particular, relative selectivities between cyclohexane and benzene were systematically changed according to the mesoporous BEA zeolites. The cyclohexane formation rate increased linearly with the increased number of Brönsted acid sites. In particular, the larger the Brönsted/Lewis ratio in the zeolite framework, the higher the formation rate toward benzene, and vice versa. The present work provides the detailed effect of acidic sites on the selective formation of C_6-cyclic hydrocarbons, such as cyclohexane and benzene. The results described in this work promote the zeolite-based solid acids supporting metal nanoparticles as potential catalyst candidates for selective C−C and C−H bond activations.

■ ASSOCIATED CONTENT

Supporting Information

Synthesis of catalytic materials, and their supplementary characterization. This material is available free of charge via the Internet at http://pubs.acs.org.

■ AUTHOR INFORMATION

Corresponding Authors

somorjai@berkeley.edu
salayoglu@lbl.gov

Notes

The authors declare no competing financial interest.

■ ACKNOWLEDGMENTS

This work is funded by The Chevron Energy Technology Company. We acknowledge support from the Director, Office of Science, Office of Basic Energy Sciences, Division of Chemical Sciences, Geological and Biosciences of the US DOE under contract DE-AC02-05CH11231. The authors acknowledge support of the National Center for Electron Microscopy, Lawrence Berkeley Lab, which is supported by the U.S. Department of Energy under Contract No. DE-AC02-05CH11231. Work at the Molecular Foundry was supported by the Director, Office of Science, Office of Basic Energy Sciences, Division of Material Sciences and Engineering, of the U.S. Department of Energy under Contract No. DE-AC02-05CH11231. K. Na thanks the financial support from Basic Science Research Program through the National Research Foundation of Korea (NRF) funded by the Ministry of Education (2012R1A6A3A03039602). We thank Prof. Peidong Yang and Prof. Omar M. Yaghi for use of the TEM and XRD instruments, respectively.

■ REFERENCES

(1) Campelo, J. M.; Luna, D.; Luque, R.; Marinas, J. M.; Romero, A. A. *ChemSusChem* **2009**, *2*, 18−45.
(2) White, R. J.; Luque, R.; Budarin, V. L.; Clark, J. H.; Macquarrie, D. J. *Chem. Soc. Rev.* **2009**, *38*, 481−494.
(3) Zheng, N.; Stucky, G. D. *J. Am. Chem. Soc.* **2006**, *128*, 14278−14280.
(4) Samant, M. G.; Boudart, M. *J. Phys. Chem.* **1991**, *95*, 4070−4074.
(5) Corma, A.; Garcia, H. *Chem. Soc. Rev.* **2008**, *37*, 2096−2126.
(6) Somorjai, G. A.; Park, J. Y. *Top. Catal.* **2008**, *49*, 126−135.
(7) Tsung, C.-K.; Kuhn, J. N.; Huang, W.; Aliaga, C.; Hung, L.; Somorjai, G. A.; Yang, P. *J. Am. Chem. Soc.* **2009**, *131*, 5816−5822.
(8) Joo, S. H.; Park, J. Y.; Renzas, J. R.; Butcher, D. R.; Huang, W.; Somorjai, G. A. *Nano Lett.* **2010**, *10*, 2709−2713.
(9) Pushkarev, V. V.; Musselwhite, N.; An, K.; Alayoglu, S.; Somorjai, G. A. *Nano Lett.* **2012**, *12*, 5196−5201.
(10) Alayoglu, S.; Aliaga, C.; Sprung, C.; Somorjai, G. A. *Catal. Lett.* **2011**, *141*, 914−924.
(11) Na, K.; Musselwhite, N.; Cai, X.; Alayoglu, S.; Somorjai, G. A. *J. Phys. Chem. A* **2014**, *118*, 8446−8452.
(12) Li, H.; Bian, Z.; Zhu, J.; Zhang, D.; Li, G.; Huo, Y.; Li, H.; Lu, Y. *J. Am. Chem. Soc.* **2007**, *129*, 8406−8407.
(13) Prieto, G.; Martínez, A.; Concepcion, P.; Moreno-Tost, R. *J. Catal.* **2009**, *266*, 129−144.
(14) Schwab, G. M.; Koller, K. *J. Am. Chem. Soc.* **1968**, *90*, 3078−3080.
(15) Boffa, A. B.; Lin, C.; Bell, A. T.; Somorjai, G. A. *Catal. Lett.* **1994**, *27*, 243−249.
(16) An, K.; Alayoglu, S.; Musselwhite, N.; Plamthottam, S.; Melaet, G.; Lindeman, A. E.; Somorjai, G. A. *J. Am. Chem. Soc.* **2013**, *135*, 16689−16696.
(17) Rinaldi, R.; Schüth, F. *Energy Environ. Sci.* **2009**, *2*, 610−626.

(18) Corma, A. *J. Catal.* **2003**, *216*, 298−312.
(19) Vermeiren, W.; Gilson, J.-P. *Top. Catal.* **2009**, *52*, 1131−1161.
(20) Corma, A.; Nemeth, L. T.; Renz, M.; Valencia, S. *Nature* **2001**, *412*, 423−425.
(21) Camblor, M. A.; Corma, A.; Martínez, A.; Pérez-Pariente, J. *J. Chem. Soc., Chem. Commun.* **1992**, 589−590.
(22) Sen, T.; Chatterjec, M.; Sivasanker, S. *J. Chem. Soc., Chem. Commun.* **1995**, 207−208.
(23) Clark, J. H. *Green Chem.* **1999**, *1*, 1−8.
(24) Bell, A. T. *Science* **2003**, *299*, 1688−1691.
(25) Burda, C.; Chen, X.; Narayanan, R.; El-Sayed, M. A. *Chem. Rev.* **2005**, *105*, 1025−1102.
(26) Zhang, W.; Smirniotis, P. G.; Gangoda, M.; Bose, R. N. *J. Phys. Chem. B* **2000**, *104*, 4122−4129.
(27) Na, K.; Choi, M.; Ryoo, R. *J. Mater. Chem.* **2009**, *19*, 6713−6719.
(28) Ayrault, P.; Datka, J.; Laforge, S.; Martin, D.; Guisnet, M. *J. Phys. Chem. B* **2004**, *108*, 13755−13763.